

Properties of Alkali Activated Slag Mortar after Exposure to Elevated Temperatures for Different Time

Tao Li¹, Ya-mei Zhang¹, Jian-guo Dai²

¹School of Materials Science and Engineering, Jiangsu Key Laboratory of Construction Materials, Southeast University
Nanjing, China

msd73196@163.com; ymzhang@seu.edu.cn

²Department of Civil and Environmental Engineering, Hong Kong Polytechnic University
Hong Kong S.A.R

cejgdai@polyu.edu.hk

Abstract - This paper presents the research on the influence of elevated temperatures and durations on mechanical properties and microstructure of alkali activated slag mortar. Results show that the compressive and flexural strength of specimens deteriorated with the increase of temperature, especially at 800 °C, the flexural strength was lost totally. The increasing duration time had negative effect on the residual flexural strength of specimens after thermal treatment. Meanwhile, X-ray diffraction, scanning electron microscopy and energy dispersive spectrometer were used to further investigate the crystal transformation and microstructural damage in the mortar after submitted to elevated temperatures. After 800 °C thermal treatment, the XRD pattern showed strong diffraction peaks of crystalline phase “Gehlenite” and the peaks of C-S-H gels disappeared. The obtained SEM/EDS results indicated that the decomposition process of alkali activated slag mortar is responsible for the deterioration of mechanical properties after exposure to elevated temperatures with different duration times.

Keywords: alkali activated slag mortar, thermal loading, duration, strength, and microstructure

1. Introduction

Great attention has been paid to the development and usage of alkali activated materials in recent decades due to their manufacturing process with lower greenhouse gases emission, energy consumption and dust pollution with respect to the manufacturing of Portland cement [1-2]. Alkali activated slag is a kind of alkali activated material which is the alkali activation of calcium-rich blast furnace slag (referred to slag hereafter unless otherwise stated) and the main reaction products are the amorphous Na-substituted C-N-S-H gels with low Ca to Si ratio. Compared with ordinary Portland cement, alkali activated slag has many advantages such as initial curing at elevated temperatures is not essential, high strength obtained at early age, good freeze-thaw resistance and chemical resistance and etc. [3-8].

It is necessary to know the performances of building material after exposed to fire or high temperatures used in civil engineering, because fire is one of the most severe environmental issues to which the structure can be exposed and it weakens the mechanical properties of building materials directly after long and intense exposure. Therefore, resistance to fire or high temperatures is an important property of building materials. Natali Murri et al. studied the high temperature behaviour of ambient cured alkali-activated materials based on ladle slag. The results showed that the ladle slag and fly ash based AAMs exhibited superior strength gains and better thermal stability than the ladle slag and metakaolin based AAMs, it may contribute to unstable C-A-S-H phases formed in the latter group of samples [9]. Zuda and Černý studied the effect of high temperatures on the length changes of two alkali-activated aluminosilicate composites with different aggregates. The composite material with electrical porcelain aggregates exhibited a better thermomechanical behaviour in comparison with composite containing quartz aggregates [10]. Rovnaník et al. studied the microstructural changes in alkali activated granulated blast furnace slag exposed to high temperatures. They found that the microstructure of alkali activated slag changed between 600 and 800 °C, when the dehydration of C-A-S-H phase completed and new phases such as akermanite started to crystallize [11].

This study presents the mechanical properties and structure changes of alkali activated slag mortar after exposure to high temperatures with different durations by means of strength tests, XRD and SEM analysis.

2. Experimental Program

2.1. Raw materials

Slag with the specific surface area of 436 kg/m² and the density of 2900 kg/m³ was used as the source material. Its chemical composition was analysed by the XRF apparatus as indicated in Table 1. The particle size distribution of GBFS, obtained by the Winner 2000A Laser Particle Size Analyzer, ranged from 0.16 µm to 100 µm with the average particle size of 11.86 µm. A mixture of industrial grade sodium silicate solution (Na₂O: 9.0 wt% and SiO₂: 27.7 wt%, water content: 48 wt%) and industrial grade sodium hydroxide pullet (>99% purity) was used as the alkali activator, of which the modulus (the dry mass ratio of SiO₂ to Na₂O) was adjusted to 1.5 through changing the dosage of sodium hydroxide. Quartz sand with the particle size distribution from 0.075 mm to 1.18 mm and the fineness of 1.7 (i.e., determined based on ASTM C136-06) was used as the fine aggregate for preparing the alkali activated slag mortar matrix.

Table 1. The chemical compositions of slag.

Composition	CaO	Al ₂ O ₃	SiO ₂	SO ₃	P ₂ O ₅	MgO	Na ₂ O	K ₂ O	Fe ₂ O ₃	Cr	Ti
%	33.3	16.9	33.4	2.35	3.77	7.0	2.0	0.16	-	-	0.61

2.2. Specimens preparation and exposure scheme

The mix proportion of alkali activated slag mortar was originated from the mix parameter optimization of alkali activate mortar (i.e., Table 2). During the mixing process of alkali-activated slag mortar specimens, the weighted amounts of sodium hydroxide and water glass were premixed with the required water and cooled to room temperature. The weighted slag and quartz sand were added into mixer and dry-mixed for 2 minutes and then mixed with the alkali activator for another 2 minutes. After scraping the stuck dry slag and quartz sand, the mortar was mixed for 1 minute to ensure the uniformity of the mixture.

The fresh mortar was cast into the cubical moulds with the dimension of 70.7 × 70.7 × 70.7 mm³ and the prismatic moulds with the dimension of 40 × 40 × 160 mm³. All specimens were demoulded after 24 hours curing in ambient laboratory condition and then cured in an environmental chamber with a temperature of 20±1 °C and a related humidity of 90 % until 26 days. Prior to the elevated temperature exposure, all specimens were moved from the environmental chamber and subjected to air dry in an environment of 20°C and relative humidity (RH) of 70±5 % for 2 days.

Except for the reference specimens (i.e., un-exposed), all other specimens were exposed in an electric furnace at a heating rate of 10 °C/min to three target temperatures, 400 °C, 600 °C and 800 °C, respectively. At each target temperature, the exposure last for a duration of 1 hour and 2 hours, respectively (i.e., Fig. 1). Afterwards, the specimens were cooled to room temperature (around 23 °C).

Table 2. The mix proportion of alkali activated slag mortar (per 1 m³).

Mix	^a <i>n</i> (%)	^b <i>M_s</i>	^c w/b	Slag (kg)	NaOH (kg)	Water glass (kg)	Water (kg)	Quartz sand (kg)
AASM	5.0	1.5		794.0	26.5	147.8	240.7	1191.0

Note: “*n*” means alkali concentration; “*M_s*” means the modulus of alkali activator, “w/b” means the water to binder ratio.

2.3. Testing procedure

The compressive and flexural strength of heated specimens were tested in accordance with ASTM C109 and ASTM C348. The reaction products of alkali activated slag are amorphous phases which show very low intensity in XRD pattern. In order to eliminate the very strong diffraction peaks of quartz in XRD pattern of alkali activate slag mortar specimens, the paste specimens were prepared with the same alkali concentration, modulus and water to binder ratio. The crystal structure of reaction products was determined by Bruker D-8 advanced X-ray diffraction (XRD) instrument with copper target (Cu, Kα). A receiving slit of 0.2 mm and bias voltage of 20kV were selected. The XRD scanner was run with a step size of 0.02°, and the scanning range from 5° to 70° (2θ). Micrographs of the heated specimens were taken on a Sirion field-emission scanning electron microscope equipped with an EDX probe. The experiments were carried out on dry specimens coated by golden powder, and an accelerate voltage of 20kV was used.

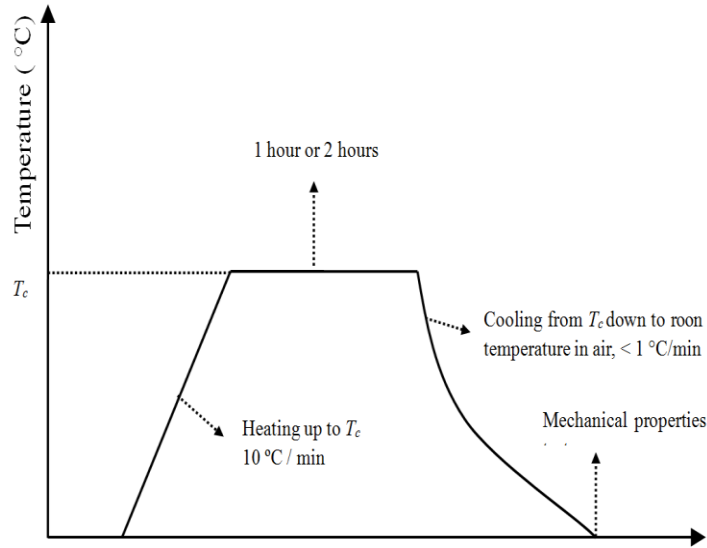


Fig. 1 Elevated temperature exposure test.

3. Test Results

3.1. Residual compressive and flexural strength

The residual compressive strength of alkali activated slag mortar after elevated temperature exposure is shown in Fig. 2. The average compressive strength of the reference specimens was 71.7 MPa. After exposure to elevated temperature of 400 °C, the strength decreased by 23.9 % - 35 %. A remarkable drop in strength was observed after exposure to 800 °C, the residual compressive strength was around 9.0 - 9.7 MPa and decreased by 87.0 % in comparison with the reference specimens.

The residual compressive strength of alkali activated slag mortars experienced 2-hour 400 °C exposure was 76.2 % (i.e., 54.6 MPa) of the unexposed mortar. This value was very similar to the residual compressive strength of specimens subjected to 400 °C exposure for 1 hours (i.e., 75.9 % of the strength of control specimens). However, an opposite trend was observed for the samples experienced 600 °C exposure. Overall, it seems that the exposure duration at a specific temperature (e.g., 1 hour and 2 hours) had no significant effect on the compressive strength degradation.

In Fig. 2, the residual flexural strength exhibits a very similar trend in temperature dependence with the residual compressive strength. The elevated temperature exposure led to decreased residual flexural strength as well. Compared with reference specimens, the exposed specimens at 400 °C and 600 °C exhibited a decreased residual flexural strength by 50 % - 56 % and 71.1 % - 76.9 %, respectively. All the samples exposed to 800 °C almost lost completely their flexural strength. The flexural strength of specimens is very sensitive to the micro cracks generated during the thermal loading. A large number of generated micro cracks may be the reason causes the more severe reduction of the flexural strength than the compressive strength. The exposure time had a certain effect on the residual flexural strength. For example, the residual flexural strength of specimens exposed to 2-hour at 400 °C was 44.2 %, while 48.1 % for the specimens experienced 1-hour 400 °C exposure. When the temperature reached 600 °C, the residual flexural strength of specimens experienced 2-hour exposure was 23.1 % of the unexposed mortar, while the specimens had 28.8 % residual flexural strength with 1-hour thermal treatment.

3.2. X-ray diffraction analysis

X-ray diffraction patterns of alkali activated slag paste specimens after elevated temperatures and duration exposure are illustrated in Fig. 3. It is well known that the main reaction products of alkali activated slag are the amorphous Al-substituted C-A-S-H gels with low Ca/Si ratio, which incorporating significant amounts of Na cations to balance the charge [12-13]. In XRD patterns of specimens after thermal treatment under 800 °C, peaks around 29° together with the basal reflections at around 32° and 50° are characteristic of C-S-H gels (PDF number of 33-0306). Besides, a very strong peak around 29.42° belongs to the diffraction peaks of calcite, which is overlapped with a nearby peak of C-S-H gels. The traces

of calcite demonstrated that carbonation happened. When the temperature is up to 800 °C, only the diffraction peaks of crystalline phase “Gehlenite” (PDF number of 33-0755) can be observed in the XRD patterns, however, the traces of C-S-H gels disappeared. In all XRD patterns no trace of wollastonite, diopside, merwinite were found, which were reported as the generated crystalline phases in alkali activated slag paste after exposure to high temperatures by Rovnaník et al [11].

Fig. 2 Residual compressive and flexural strength of specimens versus temperature.

Fig. 3 X-ray diffraction patterns of alkali activated slag mortar specimens with thermal loading.

3.3. Scanning electronic microscopy/Energy dispersive spectrometer

In order to better understand the damage process on the structural changes, a microstructural investigation using scanning electronic microscopy (SEM) was carried out. Meanwhile, the element analysis was also investigated using energy dispersive spectrometer (EDS) simultaneously. Fig. 4 shows SEM/EDS photographs of the specimens in their normal condition and after exposure to the target temperatures with different durations.

Fig. 4 clearly visualizes the difference between the structure in normal condition and after exposure to high temperatures. Fig. 4(a) presents the fracture surface of the specimen at 23 °C, amorphous reaction products of alkali activate slag containing a great number of microcracks can be observed, which were caused by very high drying shrinkage. It is one of the typical characteristics of alkali activated slag reported by previous studies [14-15]. When the temperature increased, the micro cracks became more significant, which can be verified from the comparison of SEM photographs of specimens in Fig. 4. This phenomenon was similar to the previous study [11]. Meanwhile, the increased duration time at each target temperature resulted in an increasing width of cracks, which is one of the factors deteriorating the flexural behaviour of specimens [i.e., Fig. 4(d) and Fig. 4(e)].

Except for the microcracks propagation, the changing of microstructure can also be observed. Compared with the reference matrix, the fracture surface of specimens after exposure to 400 °C with 1 hour durations presented a porous characteristic, and the morphology of reaction products changed from spherical to rod-like shape [i.e., Fig. 4(b)]. When the temperature increased to 600 °C, loose packing of a great number of small spherical particles can be found in the morphology of specimen with 1 hour duration [Fig. 4(d)]. In Fig. 4(f), a significant change of matrix morphology can be found after exposure to 800 °C following with the increasing number of larger pores, which shows a severe structural damage after thermal load.

Fig. 4 also shows the EDS trace of area marked in each morphology, the area that seems like C-S-H gels was selected. It can be found that the dominant peaks of all morphologies belong to Ca, Si, Al and Na elements. In Fig. 4 (f) and 4(g), the Ca/Si ratio of the selected area is around 0.47 and 0.56, respectively, which is much lower than the Ca/Si ratio of others specimens (around 0.7-1.3). The reason may contribute to the decomposition of C-S-H gels and the formation of crystalline phase “Gehlenite” with the chemical formula of $\text{Ca}_2\text{Al}_2\text{SiO}_7$ (i.e., test results of XRD tests).

4. Conclusion

In this paper, the mechanical properties and microstructure of alkali activated slag mortar subjected to temperatures at 400 °C, 600 °C and 800 °C with 1 hour and 2 hours duration, respectively, have been presented. From the above obtained results, the conclusions can be drawn:

- 1) The compressive and flexural strength of the alkali activated slag mortar is strongly influenced by the elevated temperature, respectively. For the residual compressive strength, the critical strength deteriorate can be found when the specimens suffered 800 °C thermal treatment. The residual flexural strength of specimens decreased higher than the residual compressive strength at the same condition. The duration time has no significant effect on the residual compressive strength of specimens after exposed to elevated temperatures. However, the residual flexural strength of specimens was deeply decreased by the increasing of duration time.
- 2) XRD results indicated that an obvious crystal transformation formed when the specimens suffered 800 °C thermal treatment with 1 hour and 2 hour durations. Only the crystalline phase of “Gehlenite” was found in the XRD pattern, and the diffraction peaks of C-S-H gels were disappeared.
- 3) Both the elevated temperatures and duration time have a significant negative effect on the microstructure of alkali activated slag mortar. The morphologies of the specimens showed a change from smooth and compactable packing to porous and loose packing. Meanwhile, the microcracks propagation was observed. The EDS results showed a decreasing trend of Ca/Si ratio. The decomposition process of alkali activated slag mortar is responsible for the deterioration of flexural behavior of panels after exposure to elevated temperatures.

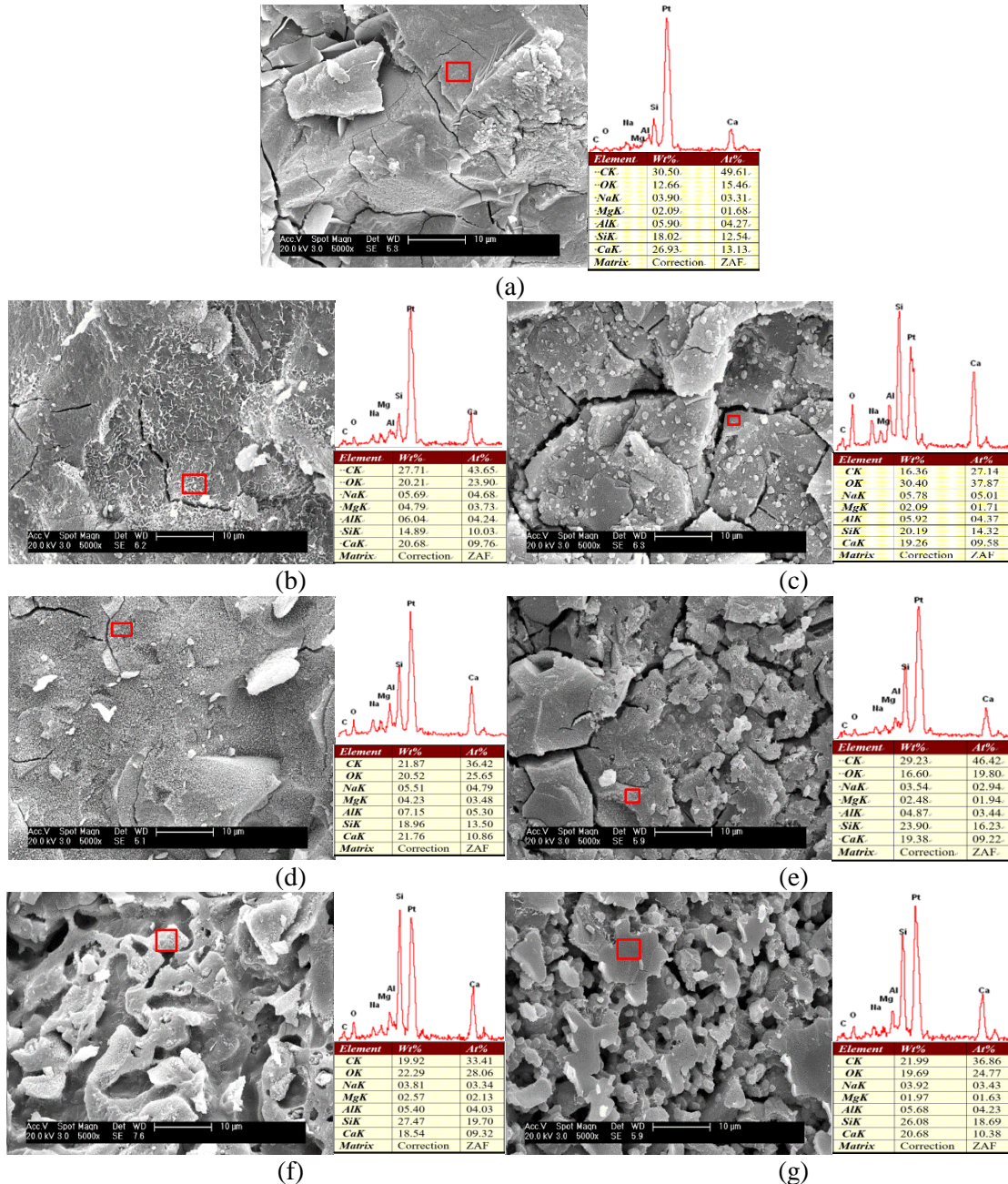


Fig. 4: SEM/EDS photographs of specimen in its natural condition and after exposure to temperatures of (a) Reference, (b) 400-1h, (c) 400-2h, (d) 600-1h, (e) 600-2h, (g) 800-1h, (h) 800-2h.

Acknowledgements

The authors would acknowledge the funding support from the National Natural Science Foundation of China (No. 51378115) and Innovation and Technology Fund of the Hong Kong SAR (No. ITF/064/12).

References

- [1] F. Pacheco-Torgal, J. Castro-Gomes, and S. Jalali, "Alkali-activated binders: A review Part 1. Historical background, terminology, reaction mechanisms and hydration products," *Constr. Build. Mater.*, vol. 22, no. pp. 1305-1314, 2008.
- [2] C. Shi, A. F. Jiménez, and A. Palomo, "New cements for the 21st century: the pursuit of an alternative to Portland cement," *Cem. Concr. Res.*, vol. 41, no. 7, pp. 750-763, 2011.

- [3] F. Pacheco-Torgal, J. Castro-Gomes, and S. Jalati, "Alkali-activated binders-A review: Part 1. Historical background, terminology, reaction mechanisms and hydration products," *Constr. Build. Mater.*, vol. 22, no. 7, pp. 1305-1314, 2008.
- [4] A. R. Brough and A. Atkinson, "Sodium silicate-based, alkali-activated slag mortars: Part I. Strength, hydration and microstructure," *Cem. Concr. Res.*, vol. 32, no. 6, pp. 865-879, 2002.
- [5] Y. W. Fu, L. C. Cai, and Y. G. Wu, "Freeze-thaw cycle test and damage mechanics models of alkali-activated slag concrete," *Constr. Build. Mater.*, vol. 25, no. 7, pp. 3144-3148, 2011.
- [6] T. Bakharev, J. G. Sanjayan, and Y. B. Cheng, "Effect of admixtures on properties of alkali-activated slag concrete," *Cem. Concr. Res.*, vol. 30, no. 9, pp. 1367-1374, 2000.
- [7] T. Bakharev, J. G. Sanjayan, and Y. B. Cheng, "Resistance of alkali-activated slag concrete to acid attack," *Cem. Concr. Res.*, vol. 33, no. 10, pp. 1607-1611, 2003.
- [8] C. Shi, "Corrosion resistance of alkali-activated slag cement," *Adv. Cem. Res.*, vol. 15, no. 2 pp. 77-81, 2003.
- [9] A. N. Murri, W. D. A. Rickard, M. C. Bigozzi, and A. Van Riessen, "High temperature behaviour of ambient cured alkali-activated materials based on ladle slag," *Cem. Concr. Res.*, vol. 43, no. 1 pp. 51-61, 2013.
- [10] L. Zuda and R. Černý, "Measurement of linear thermal expansion coefficient of alkali-activated aluminosilicate composites up to 1000 °C," *Cement and Concrete Comp.*, vol. 31, no. 4, pp. 263-267, 2009.
- [11] P. Rovnaník, P. Bayer, and P. Rovnaníková, "Characterization of alkali activated slag paste after exposure to high temperatures," *Constr. Build. Mater.*, vol. 47, no. 10, pp. 1479-1487, 2013.
- [12] M. B. Haha, B. Lothenbach, G. Le Saout, and F. Winnefeld, "Influence of slag chemistry on the hydration of alkali-activated blast-furnace slag-Part II: Effect of Al₂O₃," *Cem. Concr. Res.*, vol. 42, no. 1, pp. 74-83, 2012.
- [13] F. Puertas, M. Palacios, H. Manzano, J. S. Dolado, A. Rico, and J. Rodríguez, "A model for the C-A-S-H gel formed in alkali-activated slag cements," *J. Eur. Ceram. Soc.*, vol. 31, no. 12, pp. 2043-2056, 2011.
- [14] F. Collins and J. G. Sanjayan, "Microcracking and strength development of alkali activated slag concrete," *Cement and Concrete Comp.*, vol. 23, no. 4-5, pp. 345-352, 2001.
- [15] L. Y. Yang, Z. J. Jia, Y. M. Zhang, and J. G. Dai, "Effects of nano-TiO₂ on strength, shrinkage and microstructure of alkali activated slag pastes," *Cement and Concrete Comp.*, vol. 57, no. 3, pp. 1-7, 2015.